American Scientific Research Journal for Engineering, Technology, and Sciences (ASRJETS)
ISSN (Print) 2313-4410, ISSN (Online) 2313-4402

http://asrjetsjournal.org/

Function of Ostia in Airflow Patterns within Nasal Cavity Model with Maxillary Sinus

Erny Afiza[a]*, Yoko Takakura[b], Masahiro Iida[c]

[a,b]*Course of Science and Technology, Tokai University, 4-1-1, Kitakaname, Hadano-shi, Kanagawa, 259-1292,Japan*

[c]*School of Medicine, Tokai University, 143, Shimokasuya, Isehara-shi, Kanagawa, 259-1193,Japan*

[a]*Email: ernyafiza@yahoo.com*

[b]*Email: takakura@tokai-u.jp*

[c]*Email: tiida@is.icc.u-tokai.ac.jp*

Abstract

The variation of ostium geometry in human nose is highly debatable. The ways it affects the airflow pattern within the main nasal cavity and maxillary sinus itself remains unclear. Further studies on this matter are valuable particularly in the medical field. Therefore, the purpose of this study is to investigate the effect of ostium number, position and diameter (3~15mm) on the airflow behavior within the nasal cavity and maxillary sinus. As the results, within the maxillary sinus, the streamlines change with variation of the ostium. In case of the mass flow rate, the flow entering the sinus increases as the ostium size widened and with the presence of multiple ostia. To conclude, ostium variations especially in size and number do effects the airflow pattern particularly within the sinus itself.

Keywords: Numerical simulation; Maxillary sinus; Nasal cavity; Airflow pattern.

1. Introduction

Paranasal sinuses are air spaces located within the face bones, adjacent to the nasal airways. Besides as a weight reduction in skull, the functions of sinuses to the human body remain obscure. Many theories on the possible roles of these sinuses have been proposed such as: 1) Phonetic: to enhance the voice; 2) Respiratory: help in warming and humidifying the inhaled air; 3) Mechanical: to protect the brain, face and skull from trauma [1].

---

* Corresponding author.

Maxillary sinus, the biggest sinus, exists in pyramid-shaped space with averaged capacity of 10-15ml. It is located below the cheeks, above the teeth and on the side of the nasal cavity. The inner surface of the sinus is covered by mucosal membrane and it drains into the main nasal cavity via single or multiple openings called ostium/ostia openings. These openings (ostia) often located at the media meatus in the main nasal cavity through near the top of the maxillary sinus, which may cause difficulties in draining its content to the nasal cavity by gravity. In general, human possesses only one ostium called natural ostium with average length of about 6mm and a diameter of 1-5mm [1]. Any restriction in sinus ventilation and drainage caused by obstruction in the ostium such as clogging of the ostia, and swelling of the membrane tissue may lead to sinus related illness [2]. Having more than one ostium is also often akin to sinus diseases due to the excessive ventilation of the sinus. This will affect its efficacy in mucociliary clearance, moistening the mucosa, minimizing the pathogen access, and maintaining high concentration of nitric oxide to provide uninhabitable environment for pathogen [3,4,5]. In an attempt to understand gas exchange in maxillary sinus, C. M. Hood and his colleagues uses numerical modelling to investigate transport process between the nasal and sinus in a range of simplified models [2]. His resulting conclusion that, single ostium provides limited ventilation to the sinus, and it can be increased with the enlargement of the sinus. He also stated that, presence of more than one ostia can increased the ventilation by around four magnitude which might negatively impact the sinus health.

In other study, Ravi and his colleagues reported that the ostium size showed a significant correlation to the sinus nitric oxide level [6]. The nitric oxide level was measured within 52 patients in the nose and in the maxillary sinus. However, no data on the effect of ostium size in sinus ventilation was recorded in this study.

As the ostium is the only passage that connecting the maxillary sinus to the main nasal cavity, research on the ostium variation may lead valuable information on the comprehension of the sinus ventilation. Therefore, as an extensive from the previous research [7,8], in this study, the sinus ventilation is numerically investigated by using real-geometric models of a human nasal cavity that includes the maxillary sinus. The purpose is to clarify the morphologic role of the ostia to the maxillary sinus. Numerical experiments have been carried out on a few types of models which were created according to position, number and diameter of the ostium. The effect on the airflow pattern within the nasal cavity, maxillary sinus, and ostium have been investigated.

2. Generation of Models and Grids

A highly detailed configuration model of the human nasal cavity is fabricated, as shown in Figure 1, by the assistance of Tokai University Hospital. The three-dimensional nasal cavity model is acquired from a Computer Tomographic scan (CT scan) with spatial resolution 512x512 pixels, obtained by 0.3mm slice width.

Three shortcomings were considered in this simulation; nostril hairs, external nose shape and mucosal membrane properties. Additionally, only one side of a pair of nasal cavities is studied since the anatomy of the nasal cavities is almost identical. The data is then imported into software 3D-Slicer (by The Slicer Community) for volume rendering. Next, software 3Ds Max Design (by Autodesk inc.) is used to modify the 3D model of the nasal cavity which excludes the unwanted features such as a tongue, ethmoid sinuses, a frontal sinus and many more. Feature variations with smoothing process are also performed by using the same software. The modified model is imported through STL

data to software ICEM CFD (by ANSYS inc.) to generate the mesh before the airflow is simulated by FLUENT 14.5 (by ANSYS inc.). A few types of human nasal cavity models with and without the presence of maxillary sinus on the variation of number, position and diameter of ostia (volume: 20.6ml) were created as shown in Table 1 and Figure 3.

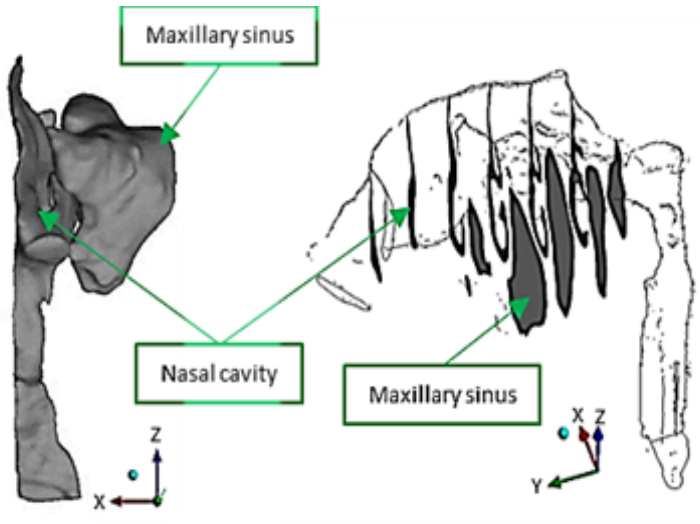

Figure 1: Nasal Cavity with Maxillary Sinus (front and isometric view)

The anterior ostium is located in the anterior/middle side of middle meatus about 42mm in Y direction from nostril (See Figure 2(a) about Y direction). Meanwhile, the posterior ostium is in the vicinity of the posterior side of middle meatus (65mm from nostril in Y direction). Model F is regarded to be the standard model with the presence of anterior ostium only which appears in more than half of healthy person.

Table 1: Variation of realistic models

Model	Ostia Features	Diameter of Ostia [mm]	Anterior Ostium	Posterior Ostium
A	Without sinus	-	-	-
B	Both Ostia	2	exist	exist
C	Anterior only	2	exist	-
D	Posterior only	2	-	exist
E	Both Ostia	3	exist	exist
F	Anterior only	3	exist	-
G	Posterior only	3	-	exist
H	Anterior only	5	exist	-
I	Anterior only	10	exist	-
J	Anterior only	15	exist	-

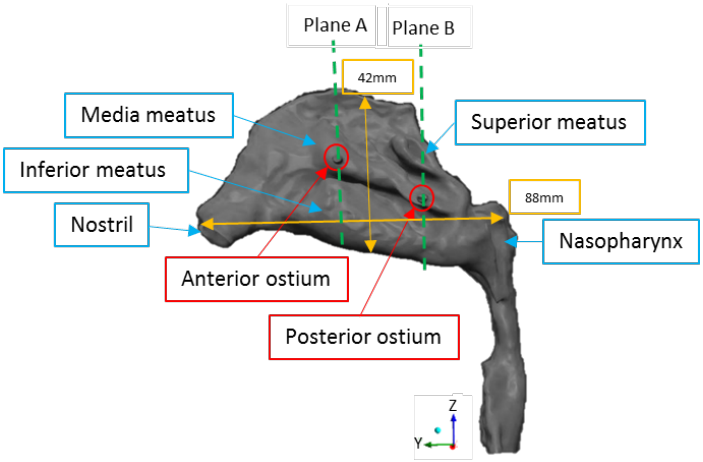

(a) Nasal cavity (Without maxillary sinus)

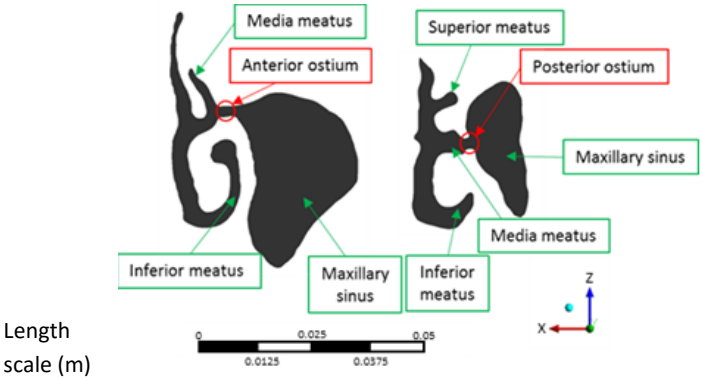

(b) Cross sectional section at Plane A (left) and B (right)

Figure 2: Structure of Nasal Cavity with Maxillary Sinus

3. Computational Condition

Experiments were carried out in Reynolds number of 1330 at the nostril area, which is obtained from the average hydraulic diameter of nares of the model at maximum breathing rate. Airflows for incompressible fluid are computed using FLUENT under the following boundary conditions: (1) The nasal wall is rigid with non-slip condition; (2) A pressure of zero (Gauge pressure) is presumed at the nostril; (3) To mimic a natural breathing airflow, user defined function is utilized to simulate unsteady condition where the maximum flow velocity of 1.9m/s is given at the trachea area. To mimic a real life breathing condition, human respiration cycle is represented by sinusoidal curve of flow rate is used in this investigation as shown in Figure 4. Periodic cycles for breathing start with the steady-state flow solution at maximum inhalation and followed by exhalation, with period time of 3 seconds in each cycle. Simulation was performed for 3 cycles (9000 time-steps), achieving a converged solution at each time-step. The third cycle was evaluated as solution during one period. In mass flow

rate at the inlet (trachea side) in responds to the time as shown in Figure 4, 1 and 2.5 seconds represent the peak inhale and peak exhale, respectively.

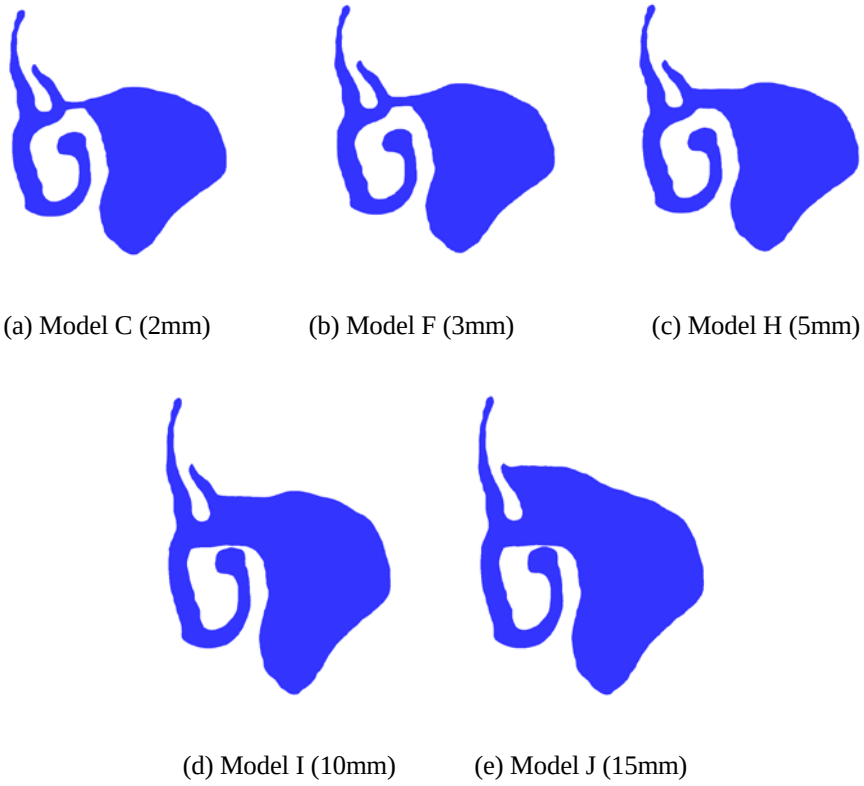

(a) Model C (2mm) (b) Model F (3mm) (c) Model H (5mm)

(d) Model I (10mm) (e) Model J (15mm)

Figure 3: Cross sectional section at plane A in Models with different anterior ostium size

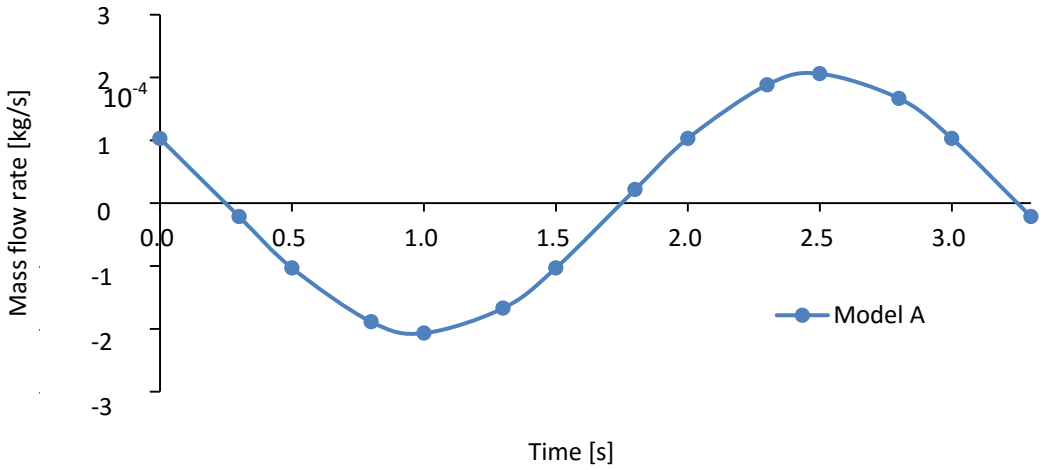

Figure 4: Respiration cycle in mass flow rate at trachea

4. Results

The airflow patterns are shown by instantaneous streamlines. For flow patterns within the sinus, streamlines passing through the plane placed at the middle of ostia are presented. Meanwhile, velocity vectors within ostia

are drawn as projection on the plane. In general, almost no discrepancy can be observed in the instantaneous streamlines within the main nasal cavity between Model A and all models with maxillary sinus despite the changes in the ostia position, number and size.

4.1 Variation of ostia position and number

In this part, since the mean diameter of ostium in healthy persons is 2.4mm, results from models 3mm are illustrated.

(a) Presence of both anterior and posterior ostia (3mm)

Instantaneous streamlines within the sinus in Model E (with both ostia) at peak inspiration and expiration is shown in Figure 5, where the red and yellow circle represents AO (anterior ostium) and PO (posterior ostium), respectively. In general, the flow is distributed in all region of the sinus during both cases of inspiration and expiration. However, discrepancy on the pattern can be observed, as the flow can be seen divided into two during inspiration and otherwise during expiration. Figure 6 (a) shows the velocity vectors in anterior and posterior ostia at peak inspiration. During inspiration, generally, the flow is introduced to the sinus through the anterior ostium, and exits at the posterior ostium. Meanwhile during expiration in Figure 6 (b), the flow enters the sinus through the posterior ostium and exits at the anterior ostium. A small vorticity occurs at the posterior ostium in the side of maxillary sinus.

(b) Presence of anterior ostium only (3mm)

With the presence of anterior ostium only, in Model F at peak inspiration, in Figure 7(a), so many streamlines cannot be detected for the same velocity magnitude as in Model E. In view of velocity vectors in Figure 8(a), the airflow generates a vortex with fairly high velocity at the ostium area, with nearly half of its velocity vectors going toward the sinus and the other half returning to the nasal cavity even before entering the sinus. Meanwhile during expiration, a flow circulates at the entrance of the anterior ostia with very small tendency of going into the sinus (Figure 8(b)), so that streamlines cannot be detected in Figure 7(b).

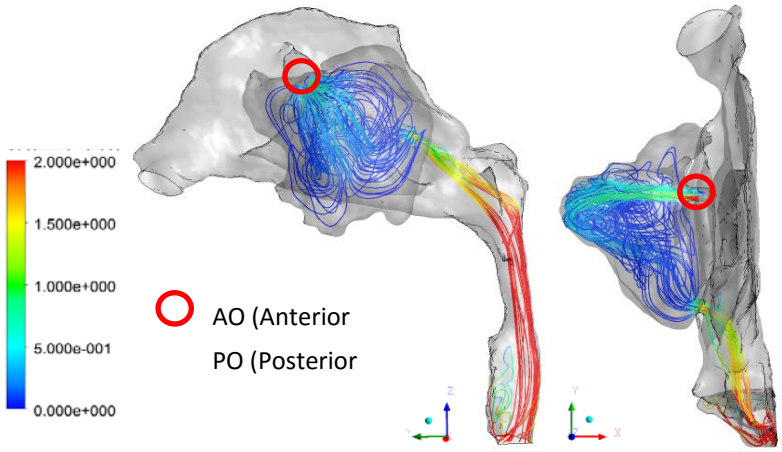

(a) Peak inspiration

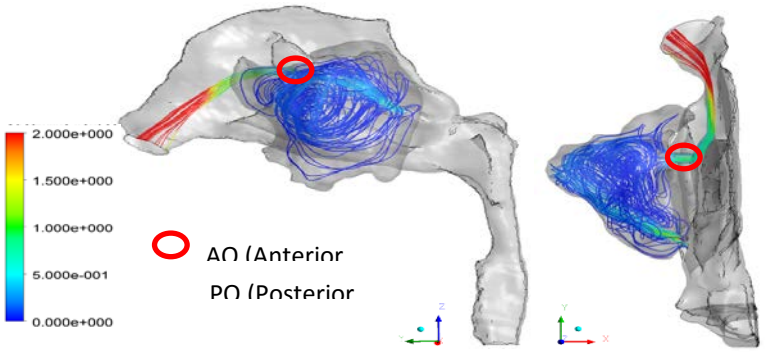

(b) Peak expiration

Figure 5: Instantaneous streamlines in sinus of Model E (side and top view)

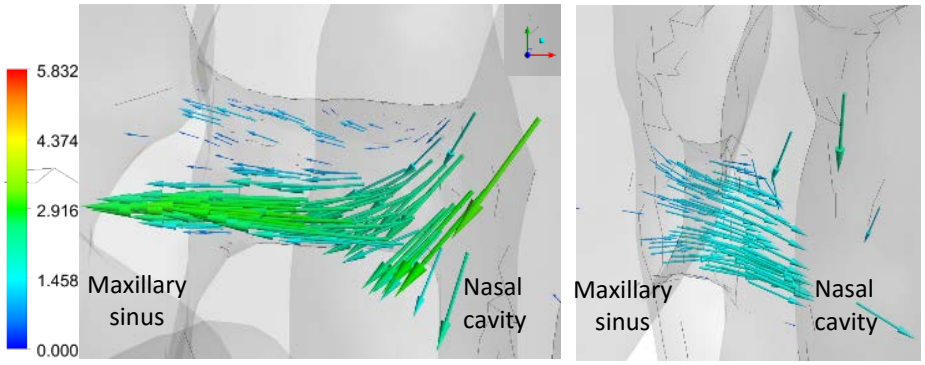

Velocity [m/s]

(a) Peak inspiration

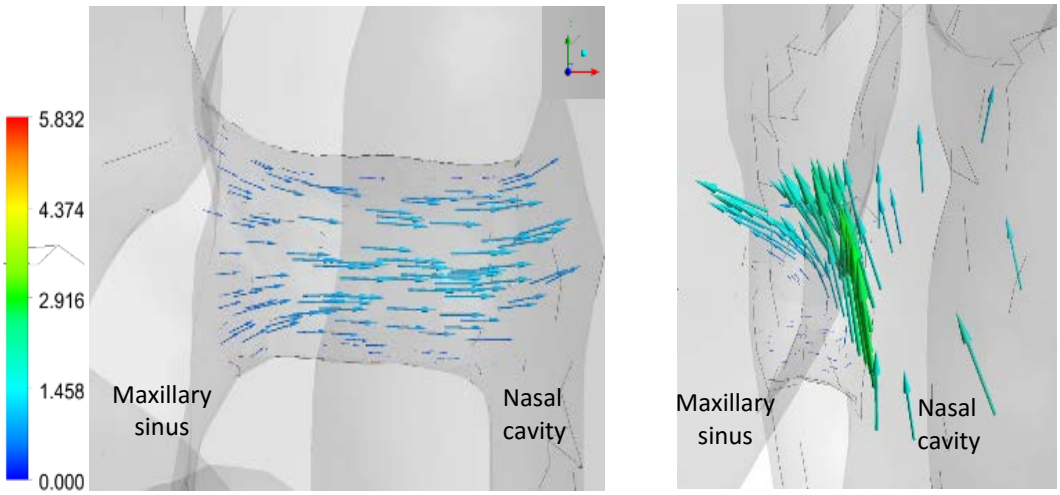

(b) Peak expiration

Figure 6: Velocity vectors in anterior (left) and posterior (right) ostia of Model E

(c) Presence of Posterior ostium only (3mm)

From Figures 9 (a) and (b), although the flow circulation area detected in Model G is larger compared to Model F, it is smaller than in Model E. As shown in Figures 10(a) and (b), during inspiration and expiration, a vortex can be observed at the ostium as the flow tends to flow into and out of the sinus. Similar to previous results, the swirl takes charge of the inflow and outflow of the ostia.

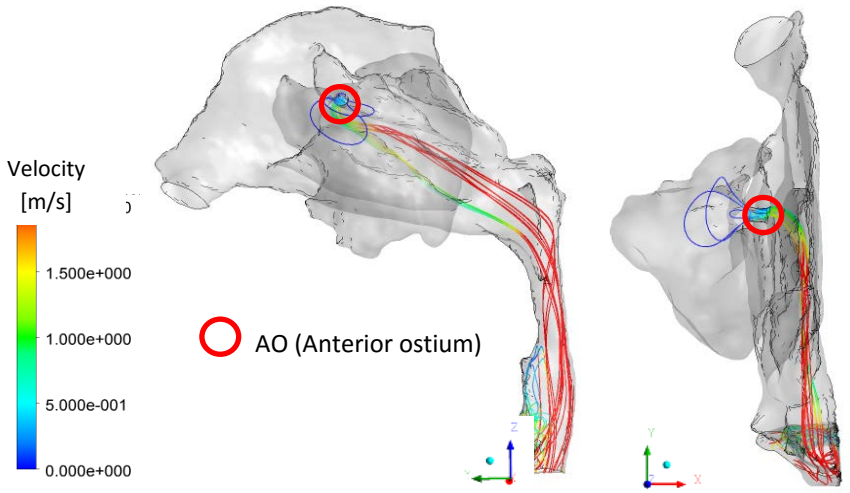

(a) Peak inspiration

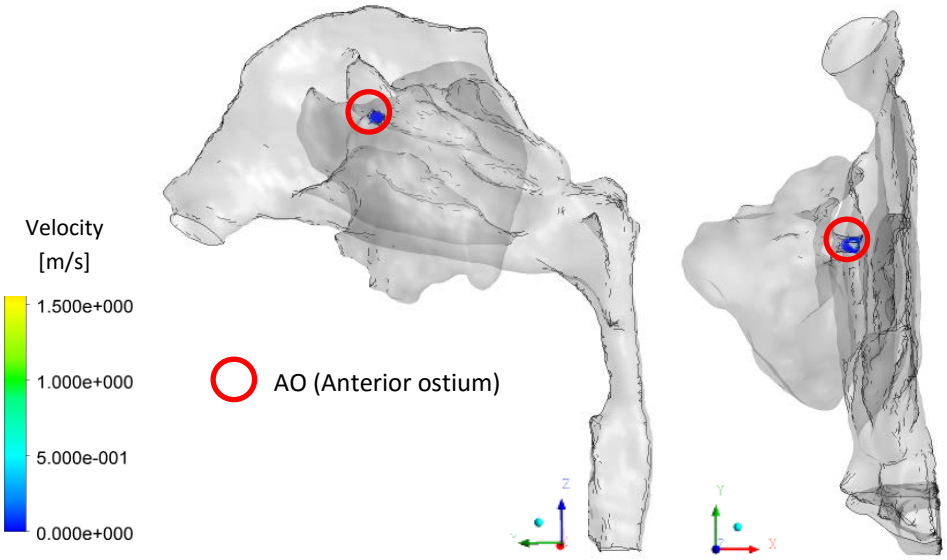

(b) Peak expiration

Figure 7: Instantaneous streamlines in sinus of Model F (side and top view)

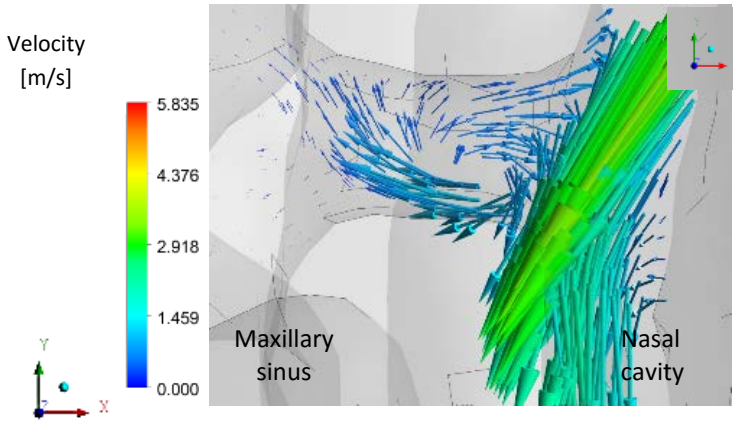

(a) Peak inspiration

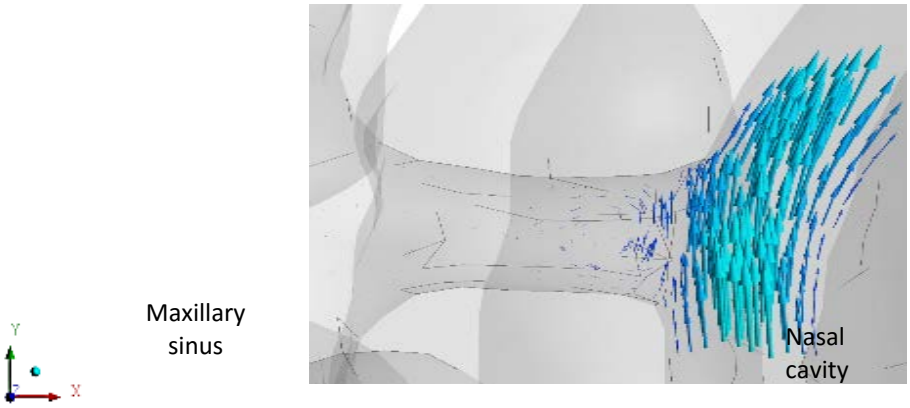

(b) Peak expiration

Figure 8: Velocity vectors in anterior ostium in Model F

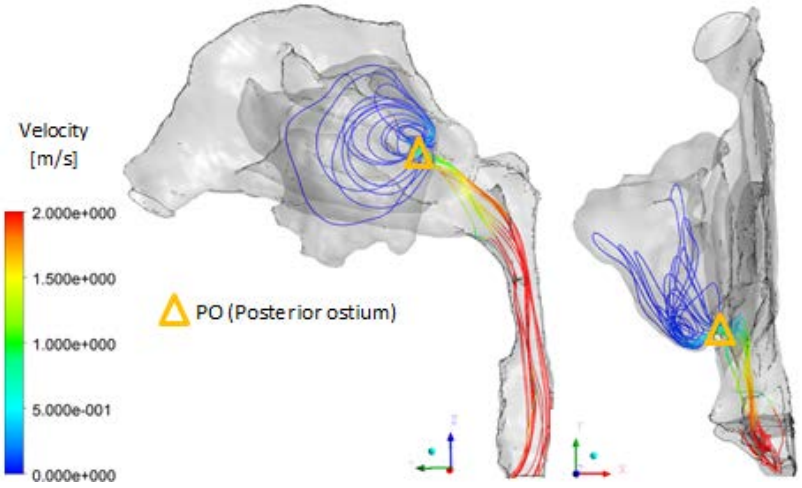

(a) Peak inspiration

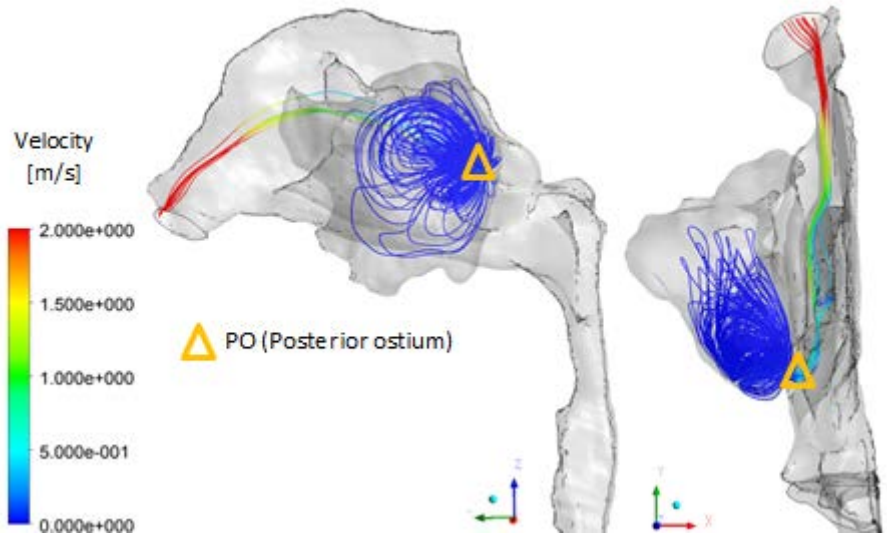

(b) Peak expiration

Figure 9: Instantaneous streamlines in sinus of Model G (side and top view)

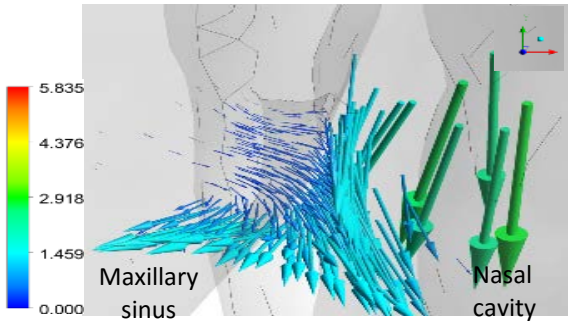

(a) Peak expiration

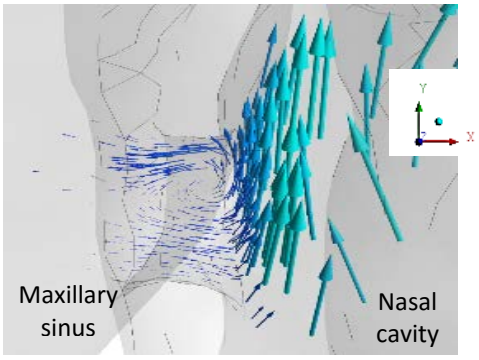

(b) Peak expiration

Figure 10: Velocity vectors in posterior ostium in Model G

Mass flow rate

Figure 11 shows the time history of mass flow rate entering the 3mm ostia. In Model E, the mass flow rate entering the sinus is at its maximum in corresponding to the peak mass flow rate at inlet in the nasal cavity model in Figure 4. However, during expiration, no obvious peak can be observed.

For models with one ostium only (Model F and G), the entering mass flow rate is much lower in comparison to that in model with both ostia (Model E). In the standard model (Model F), the entering mass flow rate takes its maximum at peak inhalation, while it remains little during expiration process. With the presence of posterior ostium only in Model G, the value is almost the same compared to Model F during inspiration, but noticeably higher during expiration.

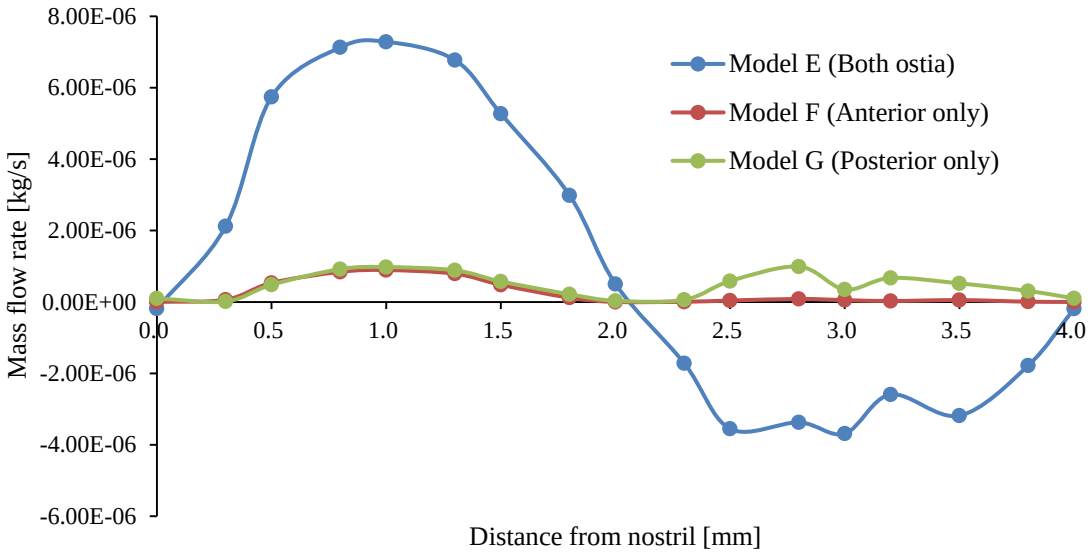

Figure 11: Mass flow rate entering sinus through mode with 3mm ostia

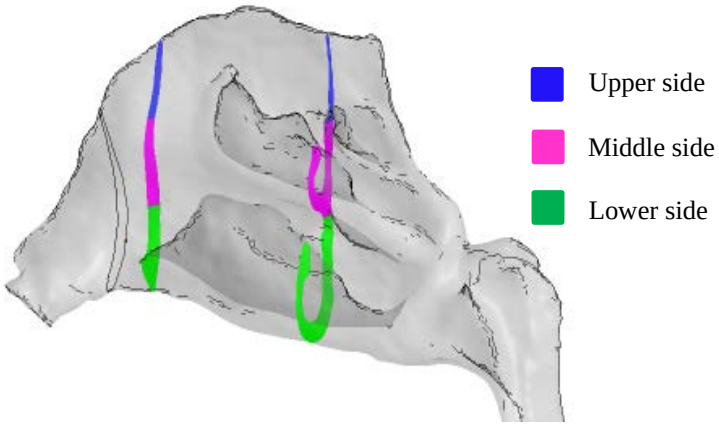

Figure 12: Description of Plane A and B in Model A

Table 2: Details of mass flow rate in Plane A

Mass flow rate in Plane A	Upper side (kg/s) (%)	Middle side (kg/s) (%)	Lower side (kg/s) (%)
Model A (without ostium)	-2.1E-06 (-1.01%)	0.000118 (57.03%)	8.96E-05 (43.25%)
Model E (both ostia)	-2.03E-06 (-0.98%)	1.17E-04 (56.58%)	9.01E-05 (43.56%)
Model F (anterior ostium only)	-2.16E-06 (-0.98%)	1.17E-04 (57.43%)	9.00E-05 (43.73%)
Model G (posterior ostium only)	-2.16E-06 (-1.05%)	1.17E-04 (57.67%)	9.00E-05 (43.46%)

Table 3: Details of mass flow rate in Plane B

Mass flow rate in Plane B	Upper side (kg/s) (%)	Middle side (kg/s) (%)	Lower side (kg/s) (%)
Model A (without ostium)	1.262E-05 (6.18%)	0.000142 (69.41%)	4.99E-05 (24.4%)
Model E (both ostia)	1.21E-05 (6.11%)	0.000138 (69.75%)	4.77E-05 (24.14%)
Model F (anterior ostium only)	1.198E-05 (5.85%)	0.000144 (70.08%)	4.93E-05 (24.07%)
Model G (posterior ostium only)	0.0000127 (6.21%)	0.000142 (69.28%)	5.01E-05 (24.5%)

In this section, the mass flow rate results were discussed quantitatively from two planes placed in the anterior side just before the flow entering the meatus region (Plane A) and in the vicinity of meatus (Plane B). To examine the local changes, these planes are divided into 3 sections, upper, middle and lower side as summarized in Figure 6.

The distribution of the mass flow rate within Plane A and B are shown in Table 2 and 3. For each plane, the middle side is the main passageway for the inhaled air, followed by lower side. Only a small quantity of flow travels through the upper side.

In Plane A, negative value of mass flow rate in the upper regions indicates that recirculation occurs in that particular area. The airflow fraction difference between middle and lower side is about 14%. The total from these two sides accounts for almost the overall mass flow rate from Plane A.

Meanwhile in Plane B, the percentage mass flow rate passes through the upper side slightly increases to about 5-6%. The value difference between middle and lower side is markedly higher in comparison to that in Plane A with about 70% in the middle and 24% in the lower side.

As for the comparison between all models, variation in the presence of ostium leaves almost no effect on the total as well as local mass flow rate as the value difference is less than 1% in all sides at both planes.

4.2 Variation of ostia size

(a) Airflow pattern

Inspiration

The instantaneous streamlines within the sinus as illustrated in Figure 13 shows that, there is a considerable difference between all models. Swirls become large and complicated along with the increment of the ostium size.

The velocity vector in the ostium area presented by Figure 14, all models show almost the same tendency where the flow enters from the posterior side of the ostium with high velocity. Meanwhile, the flow exits from the anterior side, with comparatively low velocity.

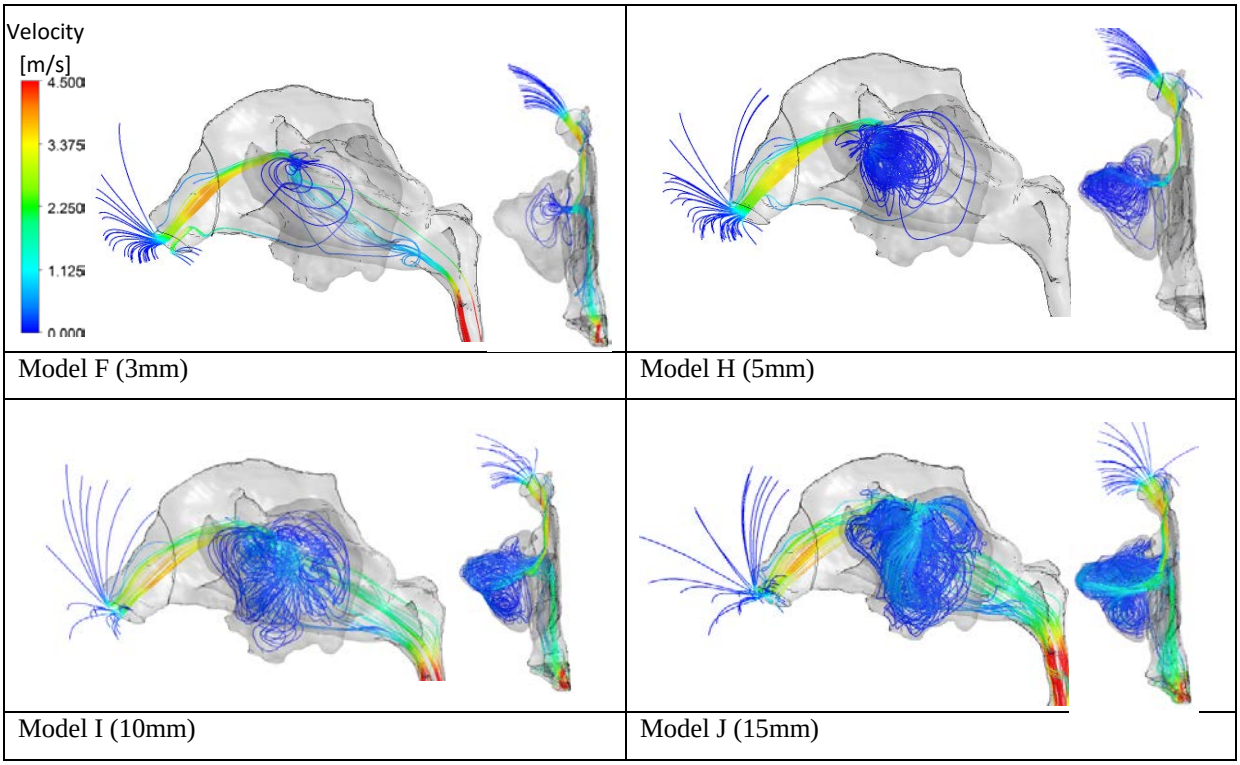

Model F (3mm) | Model H (5mm)

Model I (10mm) | Model J (15mm)

Figure 13: Instantaneous streamlines within maxillary sinus during inspiration

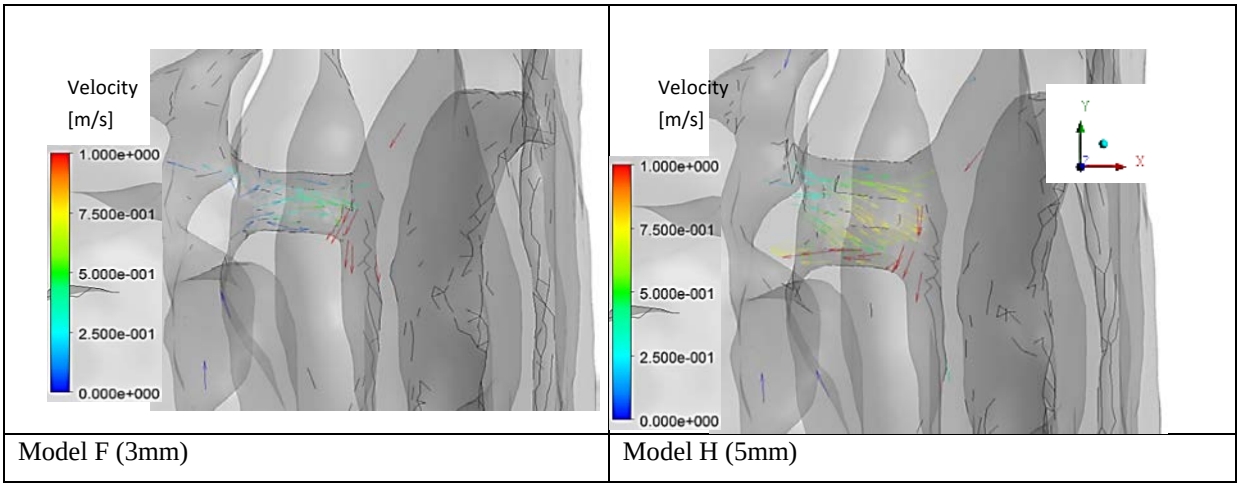

Model F (3mm) | Model H (5mm)

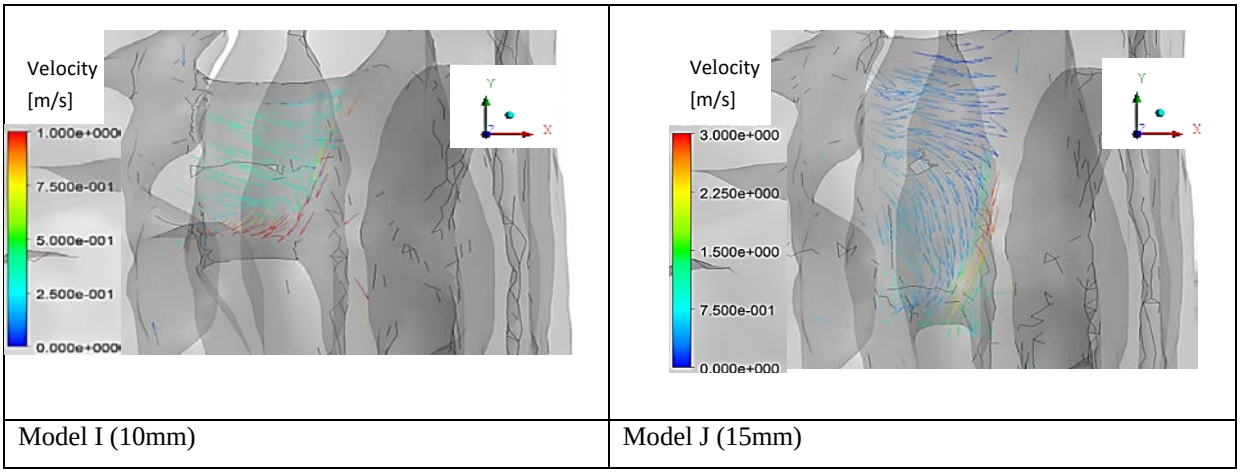

Model I (10mm)	Model J (15mm)

Figure 14: velocity vectors within ostium during inspiration

Expiration

Figure 15 illustrates instantaneous streamlines within main nasal cavity during expiration. Almost no discrepancy can be observed in airflow patterns within the main nasal cavity in all models with different ostium diameter where the mainstream is located along media and inferior meatus while exhaling. A small-scale swirl was observed at the inferior meatus at the posterior side of the cavity.

From Figure 16, in general, the streamlines in the sinus during exhaling are less complicated in comparison to that during inspiration process, where less swirls occur within the sinus itself. All models show that the same phenomenon where the flow enter the ostium directed to the anterior part of the sinus. The flow then circulates the sinus and exits through the posterior part of the ostium.

As for the airflow within the ostium, a significant inconsistency in the velocity vectors can be seen in Model F (3mm) as the flow go in and exits around the same area as shown in Figure 17. Meanwhile, in Model H (5mm) an obvious swirl occurs in the middle of the ostium, directing the flow in and out the sinus. In Model J (15mm), the velocity vector directing out of the sinus in different areas within the sinus.

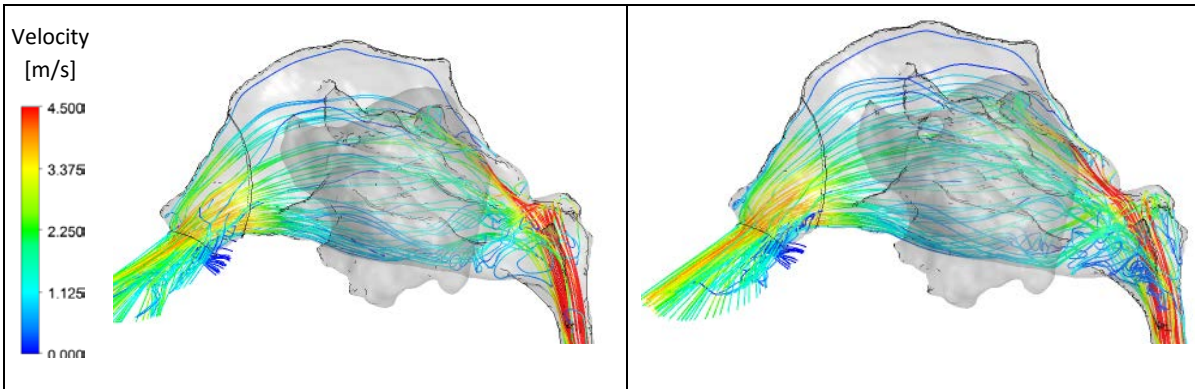

Model F (3mm)	Model H (5mm)

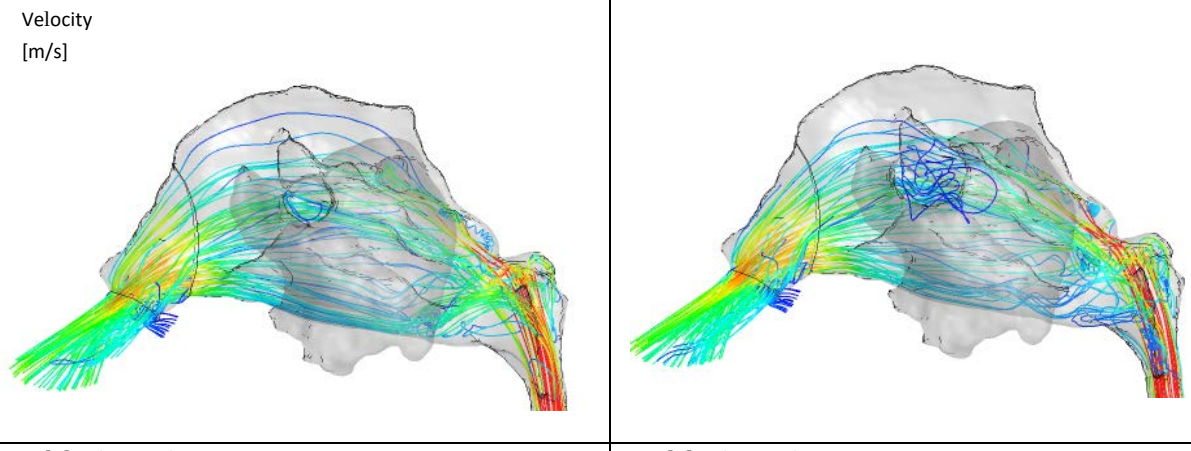

Model I (10mm)	Model J (15mm)

Figure 15: Instantaneous streamlines within main nasal cavity during expiration

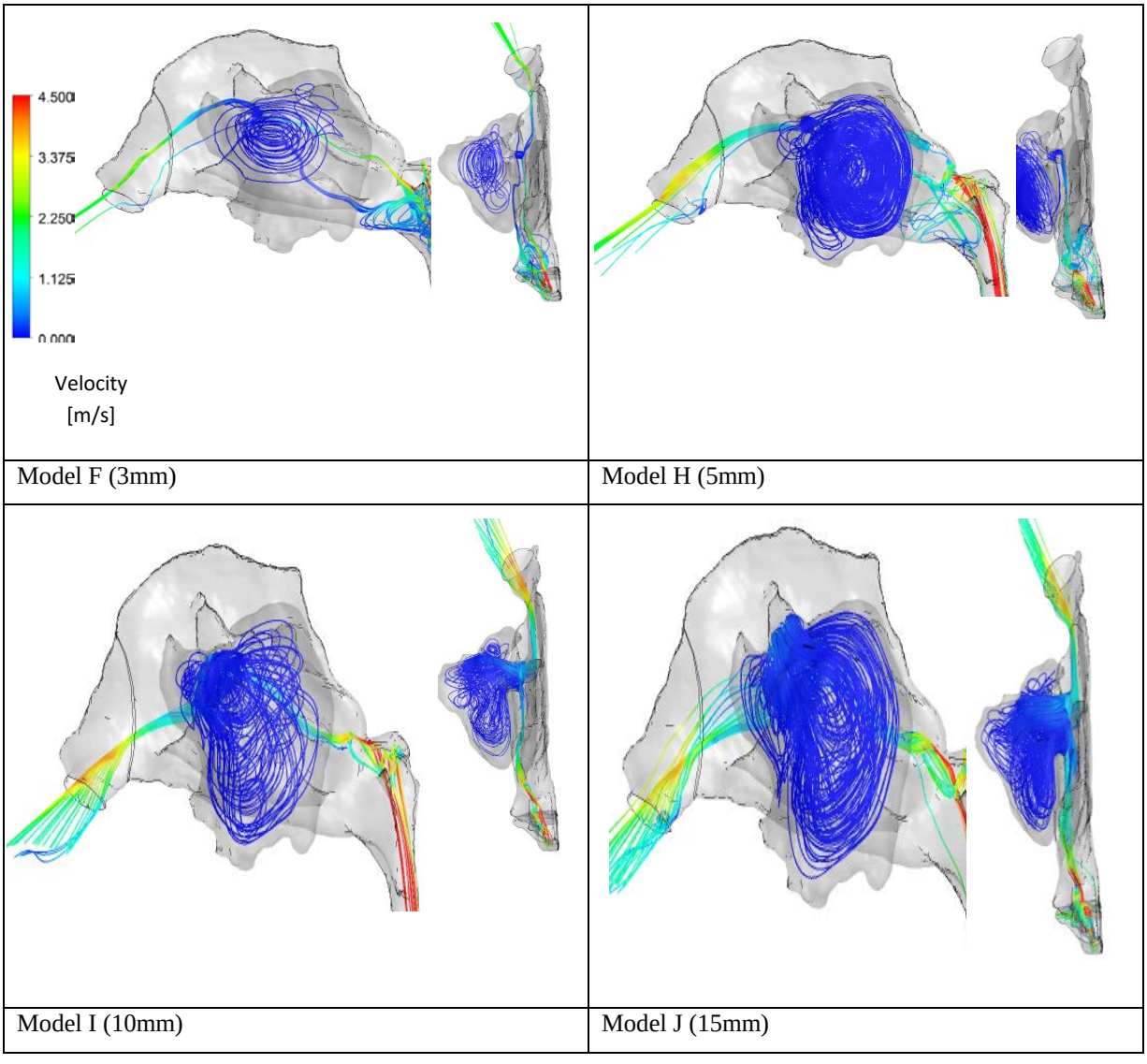

Model F (3mm)	Model H (5mm)
Model I (10mm)	Model J (15mm)

Figure 16: Instantaneous streamlines within maxillary sinus during expiration

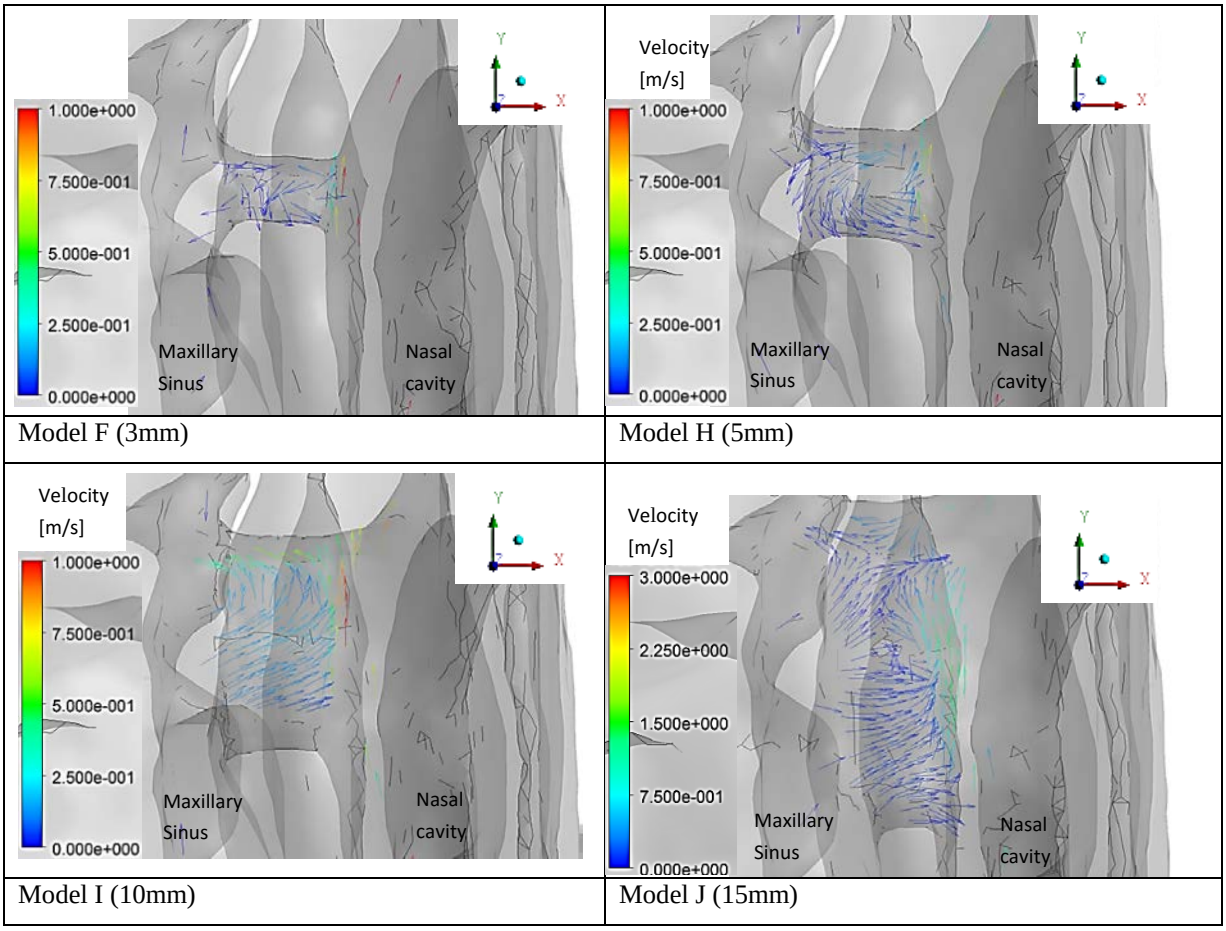

Figure 17: Velocity vector within ostium during expiration

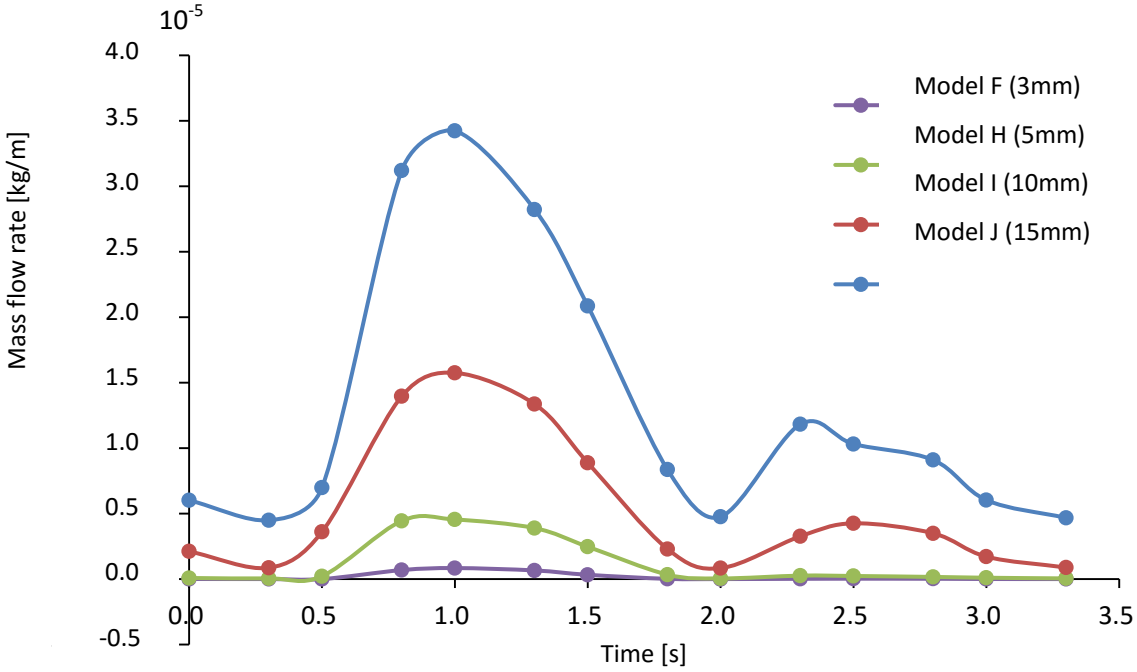

Figure 18: Time history of mass flow rate entering the sinus

Table 4: Details of mass flow rate in Plane A

Mass flow rate in Plane A	Upper side [kg/s] [%]	Middle side [kg/s][%]	Lower side [kg/s][%]
Model A (without ostium)	-2.1E-06 [-1.01%]	0.000118 [57.03%]	8.96E-05 [43.25%]
Model F (3mm)	-2.16E-06 [-0.98%]	1.17E-04 [57.43%]	9.00E-05 [43.73%]
Model H (5mm)	-2.04E-06 [-0.99%]	1.18E-04 [57.51%]	8.92E-05 [43.49%]
Model I (10mm)	-1.89E-06 [-0.92%]	1.17E-04 [57.10%]	9.00E-05 [43.82%]
Model J (15mm)	-1.20E-06 [-0.59%]	1.20E-04 [58.51%]	8.60E-05 [43.57%]

Table 5: Details of mass flow rate in Plane B

Mass flow rate in Plane B	Upper side [kg/s] [%]	Middle side [kg/s] [%]	Lower side [kg/s] [%]
Model A (without ostium)	1.262E-05 [6.18%]	0.000142 [69.41%]	4.99E-05 [24.4%]
Model F (3mm)	1.198E-05 [5.85%]	0.000144 [70.08%]	4.93E-05 [24.07%]
Model H (5mm)	1.22E-05 [5.98%]	1.41E-04 [68.66%]	5.20E-05 [25.37%]
Model I (10mm)	1.09E-05 [5.32%]	1.36E-04 [66.62%]	5.73E-05 [28.06%]
Model J (15mm)	1.50E-05 [7.37%]	1.22E-04 [60.15%]	6.61E-05 [32.48%]

Figure 18 illustrates the time history of mass flow rate entering the sinus in Models F (3mm), H (5mm), I (10mm) and J (15mm). Overall, the pattern of the mass flow rate entering the sinus is almost similar in all models, the value takes its maximum at peak inhalation, while it remains little during expiration process. Furthermore, as the ostium diameter increases, the mass flow rate entering the sinus also increases. In Model J (15mm) which possesses the largest ostium, the value is markedly larger than any other models. Meanwhile, with the smallest ostium diameter, Model F exhibits the lowest value of mass flow rate coming into the sinus.

The distribution of the mass flow rate within Plane A and B are shown in Table 4 and 5. For each plane, the middle side is the main passageway for the inhaled air, followed by lower side. Only a small quantity of flow count about 1% travels through the upper side.

In Plane A, similar to previous result, negative value of mass flow rate in the upper regions indicates that recirculation occurs in that particular area. The airflow fraction difference between middle and lower side is about 14%. The total from these two sides accounts for almost the overall mass flow rate from Plane A. A tendency can be seen in the upper side as the mass flow rate value becomes smaller long with the enlargement of the ostium, with Model A being the largest and Model J being the smallest. Meanwhile, an adverse effect was seen in middle side where Model A and E exhibit the smallest and largest flow rate, respectively. For some reasons, as the ostium becomes wide, the flow tends to flow in the upper side and less in the media side. No notable pattern can be recognized in the lower side of Plane A.

Meanwhile in Plane B, the percentage mass flow rate passes through the upper side slightly increases to about 5-7%. The value difference between middle and lower side is markedly higher in comparison to that in Plane A with about 60-70% in the middle and 24-32% in the lower side. As for the comparison between all models, variation in the presence of ostium leaves noticeable impact on the local mass flow rate especially in Model J. In the upper side in Model J, the mass flow rate percentage accounts about 7%. This difference increased in the middle side with about 10%, between Model J (largest ostium) and F (smallest ostium). Unlike in Plane A, significant change can be observed in the lower side of Plane B, as the percentage of the mass flow rate increase as the ostium size becomes large.

In the anterior part, just before the flow passed through the ostium, as the ostium size increases, the flow incline to go through the media region, while less flow in the upper region. This phenomenon might due to the high mass flow entering the sinus in larger ostium, thus, the flow is drawn to the middle region instead of to the upper area. Meanwhile, in the posterior side (after the flow passed through the ostium), with the enlargement of the ostium, more flow goes through the upper side and less in the middle side. Despite the high mass flow rate coming out from the maxillary sinus, the percentage value in the middle side of model with the largest ostium (Model J) is the lowest from any other models. Furthermore, a pattern was detected where the quantity of the flow moves through the lower side rises along with the augmentation of the ostium.

5. Discussion

In this research, the effect of the ostia variation on the airflow pattern within the nasal cavity and maxillary snus was investigated.

As for flow patterns within the main nasal cavity, almost no significant difference can be observed with or without the maxillary sinus in spite of variation of ostium position, number and diameter.

Regarding flows in the sinus with ostia variation, the followings have been obtained:

(1) Flow pattern within the maxillary sinus:

Flow patterns change with variation of number, location of ostia, and variation of ostia diameter;

(2) Mass flow rate entering the sinus:

During inhalation process, all models show the same tendency in the time history of mass flow. During exhalation process, in the standard model with an anterior ostium only (3mm), the mass flow rate is negligible, while in the model with a posterior ostium only, mass flow rate takes inconsistent tendency with that at the inlet. The value can be increased with the presence of multiple ostia and with the enlargement of the ostium;

(3) Local mass flow rate within the main nasal cavity:

Ostium enlargement causes changes in the local mass flow rate

To investigate the reliability of the present ostia models, the present results with two ostia of 3mm are compared with study with J. H. Zhu [5], where numerical simulations were carried out to assess the airflow ventilation in nasal cavity, maxillary sinus, and two ostia before and after surgery in three cases with different nasal ventilation rate: calm breathing, light breathing, and heavy breathing. Results in calm breathing were chosen to be compared with current study. Figure 20 illustrates the comparison on the sinus ventilation between both results. Both results show the similar tendency that the air entering the sinus has the maximum value at peak inspiration, while it is irregular during exhaling. In Zhu's study, the size of NO is almost the same but the size of AO is smaller in comparison to the current study, which might cause the discrepancy in magnitude of the sinus ventilation during expiration.

Thus, it has been confirmed that the present ostia models are effective to comprehend the complicated flow phenomena about the sinus ventilation.

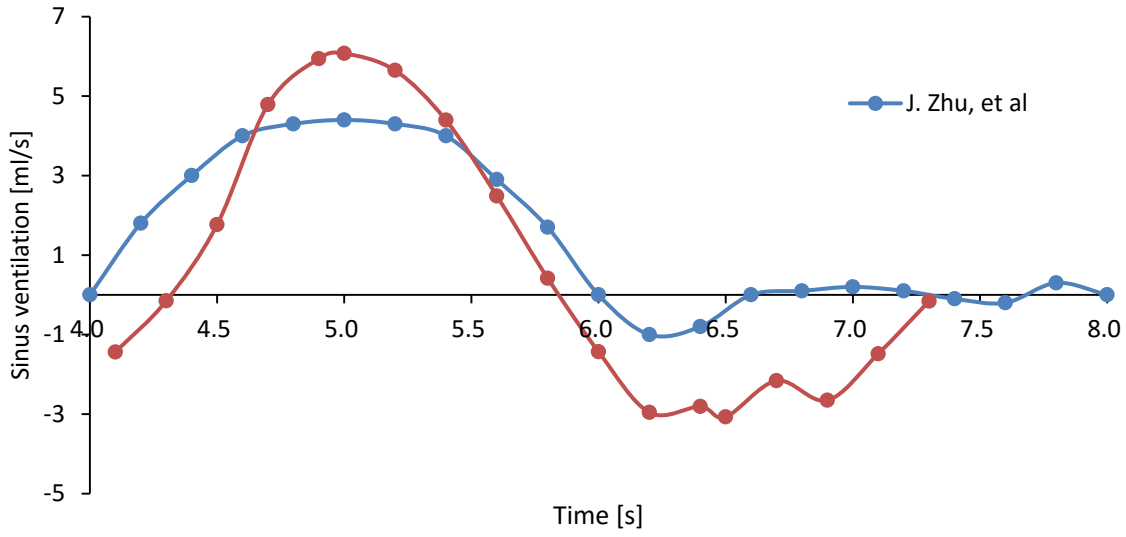

Figure 20: Comparison in sinus ventilation between present study and J. Zhu et. al.

6. Conclusion

In this study, the sinus ventilation is numerically investigated by using real-geometric models of a human nasal cavity that includes the maxillary sinus. The effect of the ostium variation on the airflow pattern within the nasal cavity, maxillary sinus, and ostium have been investigated.

The airflow within the main nasal cavity is independent with the variation of ostium position and number. The local mass flow rate in the main nasal is influenced by the changes of ostium diameter. As for the flow pattern in the maxillary sinus, the effects of the ostium variation is distinct. However, how these changes in the airflow behavior effect the maxillary sinus physiology is yet to be known.

Good ventilation in the maxillary sinus is highly debatable among the researchers as too much ventilation or blockage of the ostium may contribute negative affect to the maxillary sinus physiology. More studies on the

relevancy between the airflow pattern and the function of maxillary sinus is highly beneficial especially in the medical field.

Reference

[1] Proctor, D. F., Andersen, I., The nose: upperway physiology and the atmospheric Environment, Amsterdam. Elseveir Biomedical, (1982)

[2] Hood, C. M., Schroter, R. C., Doorly, D. J., Blenke, E. J. S. M., Tolley, N. S., Computational modelling of flow and gas exchange in models of the human maxillary sinus, J Appl Physiol, 107:1195-1203, (2009).

[3] Kane, K., Recirculation of Mucus as a cause of Persistent Sinusitis. American Journal of Rhinology and Allergy, 11:270-272, (1997a).

[4] Mathhews, B.L., Burke, A.J., Recirculation of mucus via accessory ostia causing chronic maxillary sinus diseases. Otolaryngology - Head and Neck surgery, 117: 422-423, (1997).

[5] Zhu, J. H., Lee, H. P., Lim, K.M., Gordon, B. R., Wang, D. Y., Effect of accessory ostia on maxillary sinus ventilation: A computational fluid dynamics (CFD) study, Respiratory Physiology and Neurobiology, 183: 91-99, (2012).

[6] Ravi K.D.R.A. Kirihine, M.S., Guy Rees, F.R.A.C.S., Peter-John Wormald, M.D. ,The Influence of the Size of the Maxillary Sinus Ostium on the Nasal and Sinus Nitric Oxide Levels, American Journal of Rhinology, Sept-Oct, Vol. 16, No. 5, (2002)

[7] Afiza, E., Takakura, Y., Atsumi, T., Iida, M.: Effects of ostia variation for Airflow Patterns within Nasal cavity Models with Maxillary Sinus. Journal of Medical and Bioengineering, (2015a).

[8] Afiza, E., Takakura, Y., Atsumi, T., Iida, M.: Study on ostia variation for airflow patterns within nasal cavity models with maxillary sinus, Proc. Schl. Eng. Tokai Univ., (2015b).